Diastereoselective Formation of Host–Guest Complexes between a Series of Phosphate-Bridged Cavitands and Alkyl- and Arylammonium Ions Studied by Liquid Secondary-Ion Mass Spectrometry

Alessandra Irico,[a] Marco Vincenti,*[a] and Enrico Dalcanale[b]

Abstract: The reactions occurring between a new class of cavitands that carry up to four dioxaphosphocin binding units and alkyl- and arylammonium ions was investigated by liquid secondary-ion mass spectrometry (LSIMS). As the cavitands existed as distinct diastereomers with different spatial orientation of their binding groups, these geometrical differences proved to have a dramatic influence on their chemical properties, including their ability to form host–guest complexes. In practice, only the cavitands that carry at least three P=O groups oriented toward the inside of the cavity were demonstrated to be strong ligands toward organic ammonium ions, whereas those with only two converging binding groups (either adjacent or opposite in the cavitand structure) still formed host–guest complexes, but they were much weaker. Adjacent binding sites proved to be more effective in interacting with organic ammonium ions than those lying in opposite positions. The isomers with no converging P=O groups did not act as molecular receptors. Even the isomer with one group oriented toward the inside of the cavity did not form host–guest complexes, as the absence of synergistic hydrogen bonding made the interaction from inside the cavity energetically equivalent (or even less favorable) to the outside binding. The presence in the cavitand structure of substituents with an electron-donating character proved to increase the proton affinity of the P=O binding groups and, consequently, their binding energy. The strong proton affinity of the cavitands led to the formation of stable host–guest complexes, as confirmed by the collisionally activated dissociation experiments. Effects of steric hindrance were weak, at least for the cavitands with three converging P=O groups. This confirmed that the cavity has a wide and readily accessible opening. The relative complexation constants were measured for the various guests, yielding scales of relative affinity toward each cavitand. These relative constants may represent thermodynamic values referred to the matrix used in LSIMS experiments, namely 3-nitrobenzyl alcohol (NBA), provided that kinetically controlled selvedge processes are negligible. Absolute complexation constants could not be obtained on account of the unknown pH and the protonation constant in the NBA matrix.

Keywords: cavitands · diastereomers · host–guest systems · hydrogen bonds · mass spectrometry

Introduction

The synthesis and characterization of new preorganized molecular receptors, capable of multiple noncovalent interactions with target organic molecules and ions, has been a subject of research and conveys the continuously increasing interest in recent years.[1] Among the techniques most frequently used for the characterization of noncovalent complexes formed by these interactions, nuclear magnetic resonance and mass spectrometry have played the major role as they provide clear evidence of both complex formation and arrangement, and a reasonable estimation of the interaction energetics.

The use of mass spectrometry to study host–guest and other noncovalent complexes has been recently reviewed.[2, 3] These studies can be roughly divided into two categories, namely i) those devoted to the characterization of the species formed in the condensed phase and ii) the investigations of the noncovalent interactions that may take place in the gas phase between appropriate hosts and guests.[3] While electrospray (ESI),[4] laser desorption (MALDI),[5] fast atom bombardment (FAB), and liquid secondary-ion mass spectrometry (LSIMS)[6] are the techniques most frequently utilized to isolate the noncovalent complexes from the condensed phase, ion–molecule reactions between species that are initially

[a] Prof. M. Vincenti, Dr. A. Irico
Dipartimento di Chimica Analitica
Università di Torino
Via Pietro Giuria 5, 10125 Torino (Italy)
Fax: (+39) 011-670-7615
E-mail: vincenti@ch.unito.it

[b] Prof. E. Dalcanale
Dipartimento di Chimica Organica e Industriale
Università di Parma
Parco Area delle Scienze 17/A, 43100 Parma (Italy)
Fax: (+39) 0521-905-472
E-mail: enrico.dalcanale@unipr.it

  0947-6539/01/0709-2034 $ 17.50+.50/0

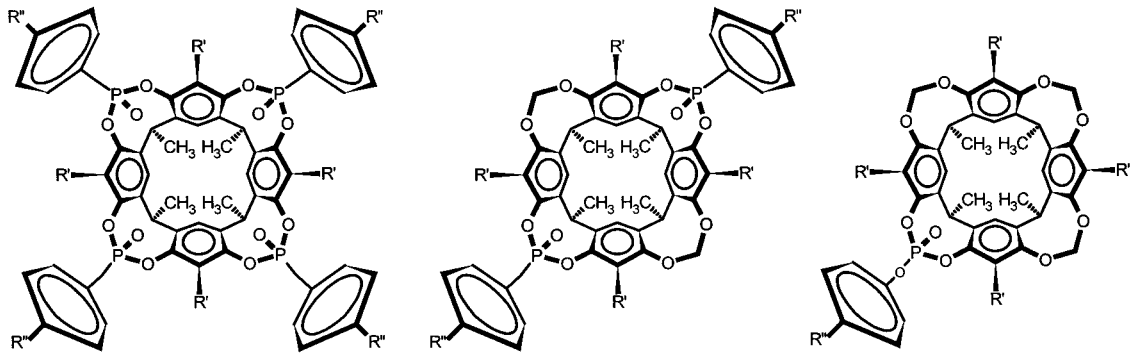

1 R' = H R'' = H
2 R' = H R'' = CH_3
3 R' = H R'' = *tert*-Butyl
4 R' = Br R'' = CH_3
Possible isomers: a, b, c, d, e, f

5 R' = Br R'' = CH_3
Possible isomers: ii, io, oo

6 R' = Br R'' = CH_3
Possible isomers: i, o

Figure 1. Cavitands investigated in the present work.

Abstract in Italian: *Si riporta lo studio effettuato mediante LSIMS delle reazioni che hanno luogo fra ioni alchil- e arilammonio e una nuova classe di cavitandi che contengono da uno a quattro gruppi fosfato a ponte. I gruppi P=O sono in grado di formare legami idrogeno con gli ioni ammonio. Poiché tali cavitandi esistono come diastereoisomeri distinti, con differente orientazione spaziale dei gruppi fosfato, si dimostra come queste differenze strutturali abbiano un'influenza spiccata sulle proprietà chimiche dei diversi diastereoisomeri, compresa la loro capacità di formare complessi di inclusione. In pratica, soltanto i cavitandi che posseggono almeno tre gruppi P=O convergenti verso l'interno della cavità manifestano forte capacità legante nei confronti degli ioni alchilammonio, mentre quelli che contengono due gruppi leganti convergenti (adiacenti o alternati) formano complessi di inclusione assai piû deboli. I gruppi P=O adiacenti mostrano migliore capacità legante dei gruppi alternati. Gli isomeri con un solo gruppo P=O rivolto verso l'interno della cavità non sono in grado di agire come recettori molecolari, in quanto l'assenza di sinergismo fra due o piû legami idrogeno rende l'interazione cavitando-ione ammonio da dentro la cavità piû sfavorevole di quella esterna. La presenza di sostituenti elettron-donatori nella struttura del cavitando aumenta l'affinità protonica del gruppo P=O e di conseguenza la sua capacità legante. L'elevata affinità protonica dei cavitandi recanti tre gruppi leganti convergenti è confermata da esperimenti di attivazione collisionale dei corrispondenti complessi. Tali cavitandi mostrano inoltre di possedere una cavità ampia e accessibile, in cui gli impedimenti sterici hanno scarsa rilevanza. Si sono determinate le costanti relative di complessazione per molte coppie di ioni ammonio, che nell'insieme hanno fornito delle scale di affinità relativa nei confronti di ciascun cavitando. Tali costanti relative rappresentano grandezze termodinamiche riferite a reazioni che avvengono nella matrice usata negli esperimenti LSIMS (3-nitrobenzil alcol). Il contributo di reazioni che avvengano in fase gas o nel "selvedge" appaiono trascurabili.*

separated are commonly performed in chemical ionization (CI) chambers,[7] ion traps,[8] and Fourier-transform ion-cyclotron resonance (FTICR) mass spectrometers.[9]

Our former research[2, 10] was mainly devoted to the study of the gas-phase reactions that occur within a CI source between large preorganized hosts (such as cavitands and bridged calixarenes) and molecular organic guests whose chemical structure prevented a preferential charging in the CI process. In other words, the poor proton affinity and electron affinity of the guests made them react as neutral species, either with neutral or charged hosts.

A novel class of cavitands that carry multiple dioxaphosphocin bridging moieties, which are capable of forming strong hydrogen bonds, has been recently synthesized.[11] The strong polar character of such substituents and their geometrical orientation make these cavitands optimal ligands for highly polar guests with which a positive charge can be partitioned. The general structure of these cavitands is provided in Figure 1. The flexible resorcin[4]arene backbone was locked into a rigid conformation by a second system of four bridges, formed by arylphosphate or O-CH_2-O units. Because of the spatial orientation of each phosphate bridge (with the P=O unit directed either inwards (i) or outwards (o) with respect to the cavity),[12] up to six different diastereomers (Figure 2) were formed with different spectroscopic and chromatographic properties which allowed their separation. The set of compounds utilized in the present work and their abbreviations are reported in Figure 1 and Table 1.

An extensive study of the spectroscopic and chemical properties of the new class of cavitands was undertaken in order to determine their selectivity toward target guests and to correlate the host–guest complex stability with the structural and configurational features of the different cavitands. The gas-phase reactivity and the interaction kinetics between these cavitands and organic amines were studied in an electrospray ionization (ESI)-FTICR mass spectrometer; the results are reported elsewhere.[13] In the present study, LSIMS was employed to investigate how the

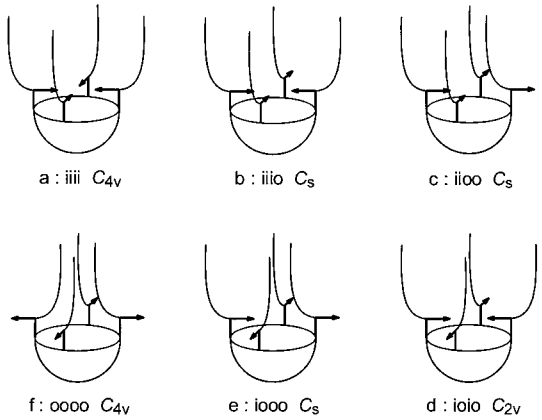

Figure 2. The six different diastereomers of cavitands **1**–**4** that arise from the spatial orientation of each phosphate bridge (with the P=O unit directed either inwards (i) or outwards (o) with respect to the cavity).

geometry of the cavitand structures and their substituents affected the chance of forming stable host–guest complexes with alkyl- and arylammonium ions.

Another objective of the present study was to compare the results obtained in LSIMS with those arising from NMR spectrsocopy[11, 14] and ESI-MS[13] in order to verify whether or not the LSIMS (or FAB) results reflected the product distribution that exists in the condensed phase. The distribution of charged host–guest complexes has been extensively used in the past to discover whether the species detected by the mass analyzer upon FAB sputtering were the result of gas-phase or condensed-phase chemistry.[15] While in most cases the scientists agreed that FAB sputters the species already present in solution (i.e., in crown ether/alkali metal ion complexes), remarkable exceptions were found for calixarenes interacting with quaternary ammonium ions,[16] a system that shares several similarities with the species studied in the present work.

Results And Discussion

Comparison of diastereomeric cavitands: The analytical characterization of various cavitands started by recording the LSI mass spectra of their positive and negative ions in different matrices. These matrices included glycerol, triethanolamine, and 3-nitrobenzyl alcohol (NBA). Although it was possible to obtain the molecular ion from all matrices and both ion polarities, it was evident that NBA provided the cleanest signal, and that ion intensities in the positive-ion mode largely exceeded those obtained in the negative-ion mode. This confirmed previous experimental findings which showed that the cavitands under study undergo efficient interaction with positively charged species. From this finding, the subsequent experiments were carried out to investigate the noncovalent interactions that occur between the cavitands and alkylammonium (and arylammonium) ions within the NBA matrix.

The first series of experiments was executed by mixing the cavitand (host, Ho) and the ammonium ion (guest, G) at a constant 1:200 molar ratio. These conditions proved optimal to favor the formation of host–guest complexes and to emphasize the different binding properties among the diastereomers. In the high-mass range, the positive-ion LSI mass spectrum of various NBA solutions exhibited the protonated cavitand $[HoH]^+$ and the adduct $[HoGH]^+$, formed by cavitand and alkylammonium ion, in widely variable relative abundance depending on the chemical structure of both species. The abundance ratio $R = [HoGH]^+/[HoH]^+$ between these two peaks is reported in Table 1 for several pairs of interacting species. It is reasonable that these abundance ratios reflect the relative ability of each cavitand and isomer to interact with the selected alkylammonium ion, even if, more precisely, for each cavitand R represents the interaction efficiency with the ammonium ion relative to that with the proton corrected by their relative concentrations and sputtering efficiencies. It should be noted, however, that the proton concentration is not known, nor are the sputtering efficiencies; however, these should not be too different from one another owing to the similar masses and structures of the protonated cavitand and its alkylammonium adduct. The R values reported in Table 1, which range from <0.1 to <100, delineate chemical systems in which either the complex is virtually absent or it is the predominant species.

Major variations of the R value occur along the diastereomeric cavitand series. A striking example of change in the distribution of the chemical species as a function of the cavitand structure is represented in Figure 3 which gives the positive-ion LSI mass spectra of diastereoisomers **2b**(iiio), **2c**(iioo), **2d**(ioio) and **2e**(iooo) interacting with the cyclo-

Table 1. Abundance ratio values (R) between the ions corresponding to the host–guest adduct ($[HoGH]^+$) and the protonated cavitand ($[HoH]^+$) in LSI mass spectra: $R = [HoGH]^+/[HoH]^+$. The cavitand concentration was 1.4×10^{-3} M; the alkyl- and arylammonium ion concentration was 0.28 M.

	1b (iiio)	**1d** (ioio)	**2b** (iiio)	**2c** (iioo)	**2d** (ioio)	**2e** (iooo)	**2f** (oooo)	**3b** (iiio)	**3c** (iioo)	**3e** (iooo)	**4b** (iiio)	**5** (ii)[a]	**5** (io)[a]	**5** (oo)[a]	**6** (i)[a]	**6** (o)[a]
m/z $[HoH]^+$	1097	1097	1153	1153	1153	1153	1153	1321	1321	1321	1465[b]	1185[b]	1185[b]	1185[b]	1045[b]	1045[b]
methylammonium			9.5	4.4	1.2	0.68	0.54	>100	99	1.1	12					
dimethylammonium	12	1.8	20	8.9	2.0	1.30	0.81	>100	>100	1.87	30	4.6	1.1	1.1	0.52	0.47
trimethylammonium			2.8	0.98	1.3	0.56	0.73	40	5.4	1.5						
2-hydroxyethylammonium	5.5	0.25	7.1	1.2	0.57	0.49	0.62	65	16	0.71						
cyclohexylammonium	7.1	1.1	11	2.8	0.98	0.67	0.83	>100	13	2.8	16	2.8	1.4	1.1	0.46	0.43
benzylammonium	6.1	0.82	9.0	2.2	1.1	0.53	0.91	>100	26	1.1						
p-toluidinium			2.7	0.58	0.25	0.21	0.32	8.0	4.7	0.14						
o-toluidinium			1.8	0.18	0.21	0.17		40	7.4	0.10						

[a] LSI mass spectra were recorded from glycerol solutions. [b] m/z values refer to the structure carrying four isotopic ^{79}Br atoms.

0947-6539/01/0709-2036 $ 17.50+.50/0 *Chem. Eur. J.* **2001**, *7*, No. 9

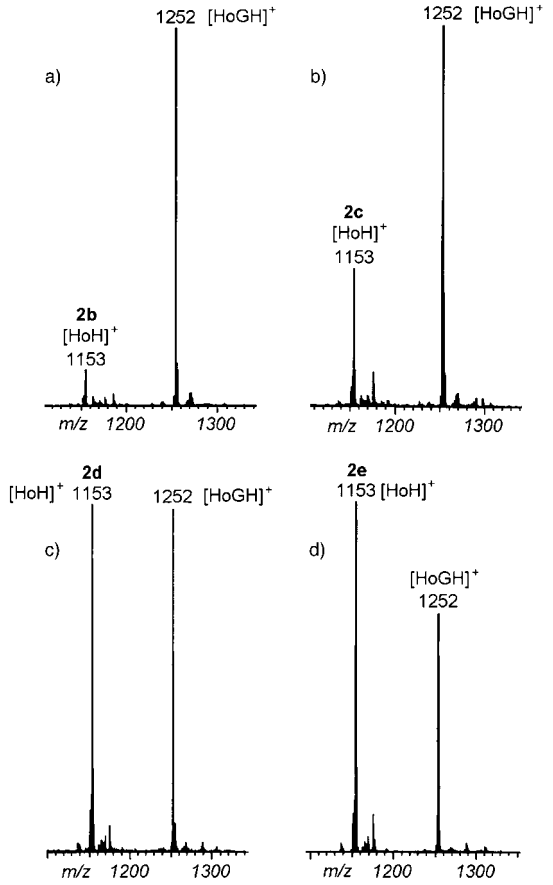

Figure 3. Positive-ion LSI mass spectra of mixtures of a cavitand (MW 1152 Da) and the cyclohexylammonium ion for various diastereomeric cavitands: a) cavitand **2b**, b) cavitand **2c**, c) cavitand **2d**, and d) cavitand **2e**.

hexylammonium ion. The protonated molecular ion of all cavitand isomers appears at *m*/*z* 1153, while the adduct formed by the cavitands and cyclohexylammonium ion gives a peak at *m*/*z* 1252. While *m*/*z* 1252 dominates the mass spectrum of Figure 3a, the relative abundance of *m*/*z* 1153 is only 10%. In Figure 3c and Figure 3d the adduct no longer represents the base peak. The same trend applies to all the other alkyl- and arylammonium ions for all series of cavitand isomers: the more P=O groups are directed inwards into the cavity, the more abundantly the adduct ion is formed. The interaction between the basic P=O groups and the ammonium ions is clearly hydrogen bonding.

There is a strong correlation between the orientation of the P=O binding groups and the formation of abundant adducts; this has been observed in ESI-MS[13] and NMR experiments.[14] These results are readily interpreted in view of the fact that three P=O groups are oriented toward the inside of the cavity in isomer **b**, while all of them are oriented outwards ($P{=}O_{out}$) in isomer **f**. The consequence is that the alkylammonium ion must be located inside the cavity of isomer **b** and outside it in isomer **f**. Thus, the adducts formed by isomer **b** are host–guest complexes, but not those formed by isomer **f**. For the intermediate isomers, other aspects should be taken into consideration including i) the size and accessibility of the cavity and ii) the occurrence of multiple and cooperative binding.

The size of the cavity varies for the different isomers as a function of the position of the aryloxy substituents on the phosphate groups. When the P=O groups are oriented toward the outside of the cavity, the corresponding aryloxy substituents project over it, reducing the cavity size (as schematically depicted in Figure 2), and partly hinder its entrance. For isomer **e**, with three aryloxy groups protruding inwards, it is unlikely that the cavity remains accessible for bulky alkylammonium ions. This is particularly true for **3e**, carrying a *tert*-butyl group on the aromatic ring. From this steric hindrance combined with the absence of converging $P{=}O_{in}$ groups capable of forming cooperative hydrogen bonds, we concluded that for isomer **e** the adduct is outside the cavity, with the ammonium ion interacting with one of the three diverging $P{=}O_{out}$ groups. This interpretation is confirmed by *R* values (Table 1) obtained for isomer **2e** interacting with the bulkier ammonium ions, which are lower than those recorded for isomer **2f** (which carries four readily accessible binding groups instead of three). Isomer **2e** produces higher *R* values than **2f** only for methyl- and dimethylammonium ions, possibly as an effect of additional interactions inside the cavity.

The presence in the cavitand structure of two or more $P{=}O_{in}$ groups offers the chance of forming multiple bonds with alkylammonium ions. In this case, more than one hydrogen is shared between the nitrogen atom of the guest and the unsaturated oxygen of the phosphate groups. Strong support for this interpretation is provided by the results obtained with the trimethylammonium ion, which has only one acidic hydrogen capable of forming hydrogen bonds: the *R* values (Table 1) obtained for this ion and cavitands **2b**, **2c**, **3b**, and **3c** are considerably lower than those observed for the same cavitands interacting with methyl-, dimethyl-, and cyclohexylammonium ions. In contrast, the *R* values obtained by cavitands **2e** and **3e** are very close to one another for all alkylammonium ions, including the trimethylammonium ion, since the isomer **e** can form only one hydrogen bond at a time, in any case.

Cavitands **2c** and **3c** exhibit *R* values compatible with multiple hydrogen bonding and strong interaction with all alkylammonium ions, although not as strong as for cavitands **2b** and **3b**. Therefore, this difference in behavior from isomers **e** is likely to be the result of cooperative binding, which can only occur inside the cavity. Thus, cavitands **2c** and **3c** form host–guest complexes and not simple adducts with alkylammonium ions. The case of cavitand **2d** is unclear: the crystal structure of **2d** (ioio) showed that the distance between the oxygens in the two opposite $P{=}O_{in}$ groups is quite large (6.29 Å).[17] Ab initio calculations for the protonated cavitand **1b** indicated that the proton is coordinated by two adjacent $P{=}O_{in}$ groups.[13] CPK models and molecular mechanics calculations also support the hypothesis that multiple hydrogen bonding is more effectively established by two adjacent $P{=}O_{in}$ groups (as in isomer **c** with iioo) than by two opposite $P{=}O_{in}$ groups (as in isomer **d** with ioio). LSIMS results confirm this interpretation, as the *R* values (Table 1) recorded for **2d** are significantly lower than those obtained for **2c**. However, partial formation of host–guest complexes by the formation of multiple bonds is confirmed by

the comparison of R values for **2d** and **2e**, the latter providing significantly lower abundance of the adduct ion than **2d**.

More selective interactions were established when the guest concentration was progressively decreased from a large excess (200-fold) to the stoichiometric amount. R values decreased proportionally with the guest concentration, as expected from solutions at thermodynamic equilibrium. At stoichiometric concentrations of cavitand and alkylammonium ion (1.4×10^{-3} M), only the isomers **2b**, **3b**, and **4b** still exhibited extensive host–guest complexation ($3 < R < 33$), whereas for the other diastereoisomers the formation of adducts with methyl-, dimethyl- cyclohexyl-, and benzylammonium ions proved negligible, with R values ranging from 0 to 1.6. The complete set of results is provided in Table 2. This data is in agreement with ^{1}H and ^{31}P NMR experiments, and indicates that only the isomer **2b** (iiio) is a strong receptor for alkylammonium ions.[14] Evidently, high guest concentrations tend to equalize the binding abilities of diastereomeric cavitands to result in comparably high R values. Thus, the presence of a pattern of three P=O_{in} groups inside the cavity produces a strong increment in the host–guest complexation constants. This effect can be ascribed to the occurrence of a three-point H-bonding motif and/or the presence of two energetically equivalent two-point H-bonding interactions.

Table 2. Abundance ratio values (R) between the ions corresponding to the host–guest adduct ($[HoGH]^+$) and the protonated cavitand ($[HoH]^+$) in LSI mass spectra: $R = [HoGH]^+/[HoH]^+$.[a]

	2b (iiio)	**2c** (iioo)	**3b** (iiio)	**3c** (iioo)	**3e** (iooo)	**4b** (iiio)
m/z $[HoH]^+$	1153	1153	1321	1321	1321	1465
methylammonium	8.0	0.10	33	0.25	0	8.1
dimethylammonium	13	0.15	23	1.5	1.6	20
cyclohexylammonium	3.3	0	17	0	0	8.7
benzylammonium	1.1	0	5.7	0	0	0.9

[a] The cavitand concentration was 1.4×10^{-3} M; the alkyl- and arylammonium ion concentration was also 1.4×10^{-3} M.

Comparison of cavitands with different chemical structures: Cavitands **1b**, **2b**, and **3b** differ from one another in their R″ groups in the *para* position of the aryloxy substituents (see Figure 1), which correspond to hydrogen, methyl, and *tert*-butyl, respectively. The effect of these substituents is significant and results in R values that increase in the order **1b** < **2b** < **3b** for all four alkylammonium ions considered. The major differences are observed for **3b**.[12] The same trend was found in ion–molecule reactions conducted in an FTICR mass spectrometer between protonated **1b**, **2b**, and **3b** with neutral amines. Here, R values and reaction efficiencies were considerably higher for **3b**.[12] It is unlikely that the increased stability of the host–guest complexes formed by **3b** arise from the steric effect of the bulky *tert*-butyl groups, as the same hindrance should be present for both the exit and the entrance of the guest. Moreover, in isomer **b** three aryloxy groups protrude from the cavity and thus leave its access quite free. Therefore, the higher reactivity of **3b** with respect to **1b** and **2b** is likely to be the result of the strong electron-donating character of the *tert*-butyl substituents that make the P=O groups more basic and stronger hydrogen-bond acceptors.

The substitution of hydrogen atoms with bromines at the upper rim of the cavity (substituent R′ in Figure 1) does not appear to have a major influence on the complexation properties of cavitands. In fact, similar R values were found for **4b** and **2b** (Table 1).

In order to study the interaction between P=O groups and ammonium ions in the absence of possible steric effects, LSI mass spectra were obtained from the cavitands of classes **5** and **6** (Figure 1) which carry two and one phosphate bridges, respectively, in the structure with methylene bridges in the remaining positions. This reduces the number of possible isomers to three for **5** [**5**(ii), **5**(io), **5**(oo)] and two for **6** [**6**(i), **6**(o)]. Brominated cavitands and their adducts yielded much weaker signals in the LSI mass spectra; however the presence of bromine substituents at the upper rim is necessary for synthetic reasons.[17] Direct comparison with tetraphosphate cavitands is not possible, not only for the structural differences, but also because glycerol had to be used instead of NBA as the LSIMS matrix to solubilize them. The isomer **5**(ii) interacts with both dimethyl- and cyclohexylammonium ions with significantly better efficiency than **5**(io) and **5**(oo), yielding R values 2–4 times higher (Table 1). This difference in R values is larger than that between cavitands **2d** (ioio) and **2e** (iooo), **2f** (oooo), and confirms the synergistic action of two converging (yet opposite) P=O_{in} binding groups. The substantial equivalence of R values for **5**(io) and **5**(oo) shows that the orientation has no effect when only one hydrogen bond can be established and no steric hindrance is present. This also excludes significant effect from additional $CH_3-\pi$ interactions. However, **5**(io) and **5**(oo) form adducts more extensively than **6**(i) and **6**(o), emphasizing the positive influence of multiple binding sites, even when the interaction with alkylammonium ions does not occur with both simultaneously.

Relative complexation constants: From R values in Table 1 it is possible to assume which alkyl- and arylammonium ion forms more stable complexes with each of the cavitands under study. A more precise comparison between two alkyl ammonium ions can be achieved under competitive conditions, namely by mixing the cavitand with an excess of two different candidate guests in equivalent concentrations. Under such conditions, the relative abundance of the peaks, corresponding to the two adducts in the LSI mass spectrum ($S = [HoG_2H]^+/[HoG_1H]^+$), approximates their relative complexation constants (the ratio of their complexation constants), provided that the sputtering efficiency in LSIMS is the same for both species. This assumption is reasonable as long as the guest is located inside the host cavity; this minimizes their different effects on both the electronic properties and the

0947-6539/01/0709-2038 $ 17.50+.50/0 *Chem. Eur. J.* **2001**, *7*, No. 9

hydrophobic character of the host–guest complexes. Two examples of these LSI mass spectra are provided in Figure 4.

By repeating these competitive complexations with different couples of alkyl- and arylammonium ions, all of them could be ordered to define a relative scale of affinity toward

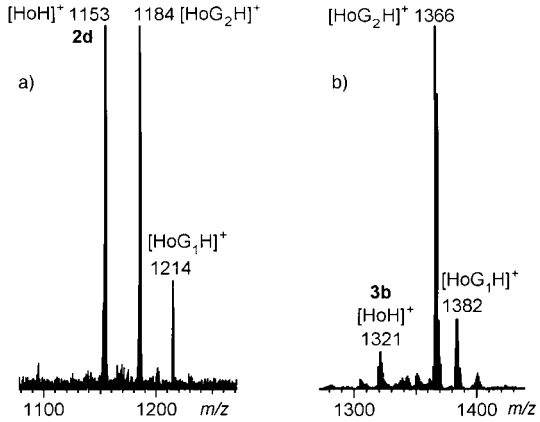

Figure 4. Positive-ion LSI mass spectra of mixtures of one cavitand and two alkylammonium ions: a) cavitand **2d** (MW 1152 Da), methylammonium ion, and 2-hydroxyethylammonium ion, b) cavitand **3b** (MW 1320 Da), dimethylammonium ion, and 2-hydroxyethylammonium ion.

the same cavitand. The numerical values we obtained varied slightly, depending on which candidate guest was selected as a common reference; however, the affinity order was maintained. These scales are reported in Table 3. Although a different affinity scale was defined for each cavitand (we tested **2b**, **2c**, **2d**, and **3b**), the order was similar. With respect to the scales that could be obtained from Table 1, there are two significant differences: from competitive complexation, it appears that i) the methylammonium ion forms more stable complexes than the dimethylammonium ion, at least with cavitands **2b** and **3b** and ii) the trimethylammonium ion forms the least stable complexes of the series. In general, the following affinity order can be established: methylammonium > dimethylammonium > cyclohexylammonium > benzylammonium > 2-hydroxyethylammonium > *p*-toluidinium > *o*-toluidinium > trimethylammonium.

Owing to the results of competitive complexations, it is clear that the most important structural feature for the formation of stable host–guest complexes is the convergence of three P=O_{in} groups to generate a multipoint hydrogen-bonding pattern. In fact, the methylammonium ion has the highest affinity and is likely to form three hydrogen bonds with cavitands **2b** and **3b**, while the trimethylammonium ion, with only one hydrogen atom available, has the lowest affinity. The second criterion that appears to determine the affinity order is the acidity of the guest. In fact, aromatic ammonium ions form less stable complexes than the aliphatic ones, and the 2-hydroxyethylammonium ion has a lower affinity than the methylammonium ion.

The analytical expressions for host protonation [Eq. (1)] and host–guest complexation [Eq. (2)] refer to the thermodynamic equilibrium established in the LSIMS matrix, namely NBA. If it is supposed that i) LSIMS data represent the equilibria occurring in the condensed phase, ii) R values represent a reasonable estimation of the concentration ratio between the host–guest complexes and the protonated host, and iii) the alkylammonium ion is in large excess with respect to the cavitand, then it is possible to derive Equation (3) which correlates experimental R values with the thermodynamic constants.

$$K_b = [HoH^+]/[Ho][H^+] \quad (1)$$

$$K_{HoG} = [HoG^+]/[Ho][G^+] \quad (2)$$

$$R = K_{HoG}C_G/K_b[H^+] \quad (3)$$

In Equations (1)–(3) Ho = Host, G = Guest, and C_G is the concentration of the guest in the LSIMS matrix. By plotting the R values as a function of C_G, it should be possible to obtain a straight line, whose angular coefficient "a" represents the ratio of the thermodynamic constants, corrected by the proton concentration [Eq. (4)]:

$$a = K_{HoG}/K_b[H^+] \quad (4)$$

Assumption i) above, which states that LSIMS data represents the equilibria occurring in the liquid LSIMS matrix has been the subject of a long-term debate.[15] If processes occurring in the gas phase (actually in the selvedge) were important in our study, then they should take place on a short timescale, that is, they should be kinetically controlled. Gas-phase interactions between protonated cavitand **2f** (oooo) and alkylamines proved to occur much faster than the corresponding host–guest complexation involving cavitand **2b** (iiio), as a consequence of the geometrical constraints associated with the entrance of the guest inside the cavity.[13] The same would apply

Table 3. Abundance ratio values (S) between the ions corresponding to two different host–guest complexes: $S = [HoG_2H]^+/[HoG_1H]^+$.[a]

G_1	G_2	**2b** (iiio)	**2c** (iioo)	**2d** (ioio)	**3b** (iiio)
2-hydroxyethylammonium	methylammonium	6.1	17	3.4	8.3
2-hydroxyethylammonium	dimethylammonium	4.5	17	3.0	5.3
2-hydroxyethylammonium	cyclohexylammonium	2.1	3.6	3.8	3.9
2-hydroxyethylammonium	benzylammonium	0.55	2.8	2.1	2.7
2-hydroxyethylammonium	2-hydroxyethylammonium	1.0	1.0	1.0	1.0
2-hydroxyethylammonium	*p*-toluidinium	0.75	0.64	0.71	1.5
2-hydroxyethylammonium	*o*-toluidinium	0.40	0.69	0.39	0.50
2-hydroxyethylammonium	trimethylammonium	0.29			
dimethylammonium	methylammonium	2.1	0.89	1.5	1.2
cyclohexylammonium	methylammonium	8.1	5.8	1.2	3.5
cyclohexylammonium	dimethylammonium	7.3	7.7	0.53	2.7
cyclohexylammonium	trimethylammonium	0.21	0.25	0.56	0.17
benzylammonium	trimethylammonium	0.48	0.48	0.54	0.54

[a] The cavitand concentration was 1.4×10^{-3} M; the alkyl- and arylammonium ion concentrations were 0.28 M.

to our case, for kinetically controlled selvedge processes. As the opposite was observed (**2b** reacts much more extensively than **2f**), we deduce that the complexation is under thermodynamic control and that the LSIMS results are likely to represent the equilibria occurring in the liquid phase.

Equation (3) was tested for the reaction of cavitand **2c** (iioo) with the dimethylammonium ion. A straight line was actually obtained with angular coefficient of 78 $mol^{-1}L$. Attempts were subsequently made to change this angular coefficient by adding nitric acid at various concentrations to the NBA matrix, without success. Upon addition of acid, the absolute intensity of the $[HoG^+]$ and $[HoH^+]$ peaks in the LSI mass spectra changed significantly; however, their ratio R remained constant at constant guest concentration. The angular coefficient did not vary substantially ($68 < a < 82$ $mol^{-1}L$).

Furthermore, in the absence of the guest, the absolute intensity of the $[HoH^+]$ peak was virtually unaffected by the presence of a relatively high concentration of nitric acid. It is deduced that the molar fraction of the protonated host in the NBA matrix must be out of the pH range where it can vary substantially, that is, it is either close to unity or close to zero. Several factors make the first hypothesis more likely: i) the dielectric constant of NBA is not known; however, it should be higher than those of benzyl alcohol (13) and nitrobenzene (35), the latter has a relatively high value;[18] ii) the autoprotolysis constant for NBA is not known either, but it should not be far from 10^{-14}, as for any other LSIMS matrix;[19] iii) the hydroxyl group of NBA has acidic character, imparted by the electron-withdrawing effect of the nitro group, which enhances the proton affinity of the substances solubilized in it; iv) the proton affinity of the cavitands that carry at least two converging $P{=}O_{in}$ groups is likely to be high because of the synergistic effect of the basic sites.

Collision-induced dissociation: A confirmation of the large proton affinity of cavitand **2b** was gained from measurements in the gas-phase by means of Cooks' "kinetic method".[20] This method requires that proton-bound dimers are formed between two different bases in the ion source of a tandem mass spectrometer. The dimeric cation is subsequently mass-selected and dissociated by collisional activation. The relative abundance of the two protonated bases in the product-ion spectrum defines their relative proton affinity.

We conducted preliminary tests of the gas-phase proton affinity of a reference compound, namely triphenylphosphate, in which the P=O group is linked to three aryloxy substituents. Triphenylphosphate represents a model, since the binding group is practically the same as in the cavitands under study; however, no inclusion complexes can be formed. Triphenylphosphate was vaporized into the ion source and treated with an amine under chemical ionization conditions. Upon collisional activation of their proton-bound dimer, the resulting product-ion spectra contained three peaks: the residual dimer and the two protonated species. The peak ratio between protonated triphenylphosphate and protonated amine were the following: ethylamine (0.26), 2-chloropyridine (0.82), and *p*-anisidine (1.25). By bracketing the gas-phase proton affinity of 2-chloropyridine (900.9 $kJ\,mol^{-1}$)[21] and *p*-anisidine (900.3 $kJ\,mol^{-1}$)[21], the proton affinity of triphenylphosphate was calculated to be 900.6 $kJ\,mol^{-1}$. This value is considerably lower than those of ethylamine (912.0 $kJ\,mol^{-1}$)[21] and any other alkylamine.

The proton-bound dimer between cavitand **2b** and an amine coincides with their protonated host–guest complex $[HoGH^+]$. It was generated by two methods: the usual LSIMS experiment with alkylammonium ions and by vaporizing the cavitand from a desorption chemical-ionization probe in the presence of the corresponding amine under CI conditions. The collisional spectra were identical, no matter which method was used to generate the dimer. The fragment ion MS/MS spectrum for the complex between **2b** and the cyclohexylammonium ion is depicted in Figure 5. From the

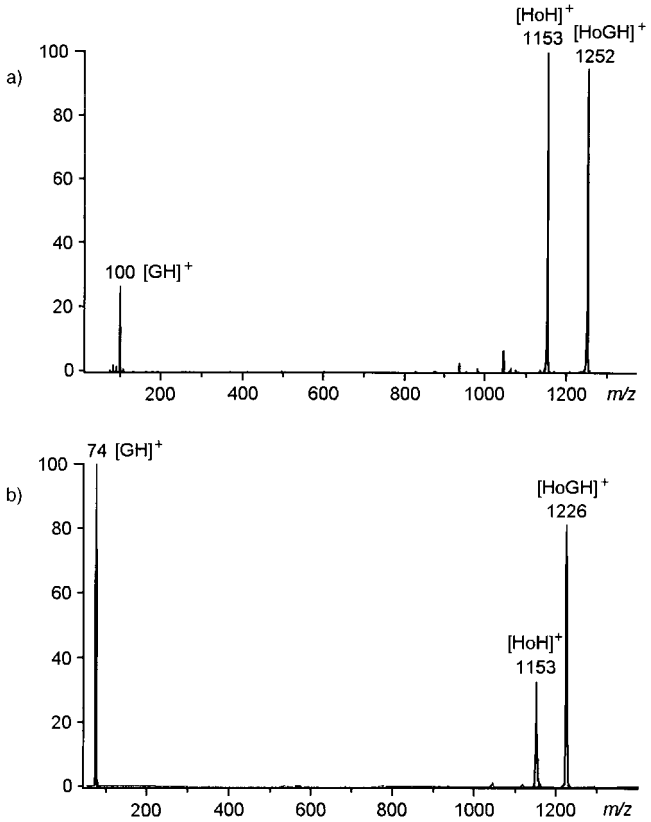

Figure 5. LSIMS/MS fragment-ion spectra of host–guest complexes formed by a) cavitand **2b** and cyclohexylammonium ion, and b) cavitand **2b** and the diethylammonium ion.

much larger abundance of the peak at m/z 1153 with respect to that at m/z 100 (peak ratio 4.15), it is evident that the cavitand **2b** retains most of the protons. On the other hand, the fragment ion spectrum of the complex between **2b** and diethylammonium exhibits a larger peak for the protonated amine than for the protonated cavitand (peak ratio 0.37). This data is provides evidence that the proton affinity of **2b** largely exceeds that of cyclohexylamine (934.4 $kJ\,mol^{-1}$)[21], but is lower than that of diethylamine (952.4 $kJ\,mol^{-1}$)[21], and is $\approx$945 $kJ\,mol^{-1}$. However, it is worth noting that the kinetic method applies only to those systems that have similar transition states and similar activation energies for the two competing dissociation reactions. This is certainly not the case for the proton-bound host–guest complexes considered, as the release of the neutral cavitand implies the dissociation of

0947-6539/01/0709-2040 $ 17.50+.50/0 *Chem. Eur. J.* **2001**, *7*, No. 9

multiple hydrogen bonds, and the geometrical rearrangements for the two processes are considerably different. Despite these limitations, CID experiments definitely support the hypothesis that the occurrence of multiple hydrogen bonding inside the cavity strongly enhances the proton affinity of the single phosphate groups and allows the cavitands (at least the **b** isomers) to favorably compete with alkylamines for protonation. The strong proton affinity of isomers **b** make their interaction with alkylammonium ions highly favorable and exothermic, as it determines extensive delocalization and sharing of the charge involved in the hydrogen bonds.

Conclusions

LSIMS experiments allowed a clear characterization of the phosphate-bridged cavitands described in the present study, in terms of their general reactivity and correlation between their structural features and their ability to form host–guest complexes with organic cations.

It was determined that: i) the binding properties of the cavitands can be almost entirely attributed to hydrogen-bonding interactions between the P=O units and alkyl- and arylammonium ions; ii) the interaction strength markedly depends on the number and pattern (adjacent–opposite) of cooperative hydrogen bonds that the two counterparts can establish, which in turn depends on the specific diastereomeric cavitand considered; iii) the interaction strength is also directly correlated with the proton affinity of both interacting species (the cavitand and the conjugated amine of alkylammonium ions were considered). Further structural aspects appear to have an influence on the stability of the complexes. The most important general feature is the rigidity of the cavitand structure. As for other systems, whose host–guest complexes could be observed in the gas phase,[2, 3, 10] the cavitands considered here also have an extremely rigid structure, which locks the binding groups into fixed positions and confers selectivity to their interactions. Moreover, the disadvantage of flexible cavitands is likely to be associated with the large entropy loss connected with the formation of host–guest complexes that reduces this flexibility, while complexations involving already rigid cavitand conformations do not have this negative entropic change.

Although obtained for different scopes, the LSIMS results were perfectly consistent with NMR[11, 14] and ESI-MS[13] data. This does not represent a definite demonstration that LSIMS results reflect the equilibria occurring in the liquid matrix; however, they are nevertheless in agreement with this hypothesis. ESI-MS, NMR, and LSIMS data support each other in defining the chemical properties of this class of cavitands and the remarkable reactivity differences occurring among diastereomeric species.

Another important outcome of the LSIMS complexation experiments is their actual value in predicting the behavior of phosphate-bridged cavitands as molecular receptors in analytical applications.[22] In this respect, the exploitation of the molecular recognition properties of this class of cavitands as supramolecular sensors[23] for the detection of ammonium ions in water is currently under study.

Experimental Section

General: All syntheses were carried out in an argon atmosphere. THF was distilled from Na/benzophenone. All chemicals were of reagent grade and used without further purification. ^{1}H and ^{31}P NMR spectra were recorded on a Bruker AMX 400 spectrometer at 400 and 161.9 MHz, respectively. Residual solvent protons were used as internal standard and chemical shifts are given relative to tetramethylsilane (TMS). Chromatography was performed on silica gel (SiO_2, Merck, 0.063–0.2 mm). Preparative TLC employed 2 mm-thick glass-backed silica-gel plates. Melting points were detected with a electrothermal melting point apparatus and are uncorrected. Elemental analyses were performed by the service of the University of Parma (Italy). The syntheses and characterization of cavitands **2**, **3**, **4**,[11] **5**, and **6**[17] have been described elsewhere.

Cavitands 1b–1d: Phenyl dichlorophosphate (6.6 mL, 44 mmol) diluted in dry THF (50 mL) was added dropwise over 1 h to a stirred solution of *rccc*-tetramethylresorcin[4]arene (3 g, 5.5 mmol) and triethylamine (12 mL, 88 mmol) in dry THF (150 mL). The reaction mixture was stirred for 8 h at room temperature. The solid triethylammonium chloride formed was filtered off and washed with THF (50 mL). The solvent was removed under vacuum, and the residue was purified by column chromatography (silica gel, CH_2Cl_2/acetone 94:6) to give four isomeric products in 60% overall yield. **1d** (ioio) white solid, TLC: $R_f = 0.70$; **1b** (iiio) white solid, TLC: $R_f = 0.60$. Isomers **1c** (iioo) and **1e** (iooo) were eluted together ($R_f = 0.50$) and were not purified further.

Cavitand 1b (isomer iiio): M.p. $> 300\,^\circ$C; ^{1}H NMR (400 MHz, $CDCl_3$): $\delta =$ 1.85 (pseudo t, ^3J (H,H) = 7.4 Hz, 12H; CH_3), 4.85 (dq, ^3J (H,H) = 7.4 Hz, ^5J (H,P) = 2.3 Hz, 2H; C*H*-CH_3), 4.93 (m, 2H; C*H*-CH_3), 6.55 (t, ^4J (H,P) = 1.4 Hz, 2H; ArH), 6.88 (t, ^3J (H,H) = 7.7 Hz, 1H; PhH_p), 6.90 (t, ^4J (H,P) = 1.6 Hz, 2H; ArH), 6.98 (t, ^3J (H,H) = 7.7 Hz, 1H; PhH_p), 7.15 (t, ^3J (H,H) = 7.7 Hz, 2H; PhH_p), 7.23–7.42 (m, 20H; ArH, PhH_m, PhH_o); ^{31}P NMR (161.9 MHz, $CDCl_3$): $\delta = -18.50$ (s, 2P, PO_{in}), -18.55 (s, 1P, PO_{in}), -26.26 (s, 1P, PO_{out}); MS (NBA, FAB): *m*/*z* (%): 1097 (100) $[M+H]^+$; elemental analysis calcd (%) for $C_{56}H_{44}O_{16}P_4$ (1096.8): C 61.32, H 4.04; found C 61.12, H 4.35.

Cavitand 1d (isomer ioio): M.p. $> 300\,^\circ$C; ^{1}H NMR (400 MHz, $CDCl_3$): $\delta =$ 1.82 (d, ^3J (H,H) = 7.3 Hz, 6H; CH_3), 1.88 (d, ^3J (H,H) = 7.3 Hz, 6H; CH_3), 4.84 (dq, ^3J (H,H) = 7.3 Hz, ^5J (H,P) = 2.5 Hz, 2H; C*H*-CH_3), 5.00 (dq, ^3J (H,H) = 7.3 Hz, ^5J (H,P) = 3.0 Hz, 2H; C*H*-CH_3), 6.60 (t, ^4J (H,P) = 1.7 Hz, 4H; ArH), 6.93 (m, 6H; PhH_o, PhH_p in), 7.05 (m, 4H; PhH_m in), 7.19 (m, 6H; PhH_o, PhH_p out), 7.34 (m, 4H; PhH_m out), 7.40 (s, 4H; ArH); ^{31}P NMR (161.9 MHz, $CDCl_3$): $\delta = -17.66$ (s, 2P, PO_{in}), -26.28 (s, 2P, PO_{out}); MS (NBA, FAB): *m*/*z* (%): 1097 (100) $[M+H]^+$; elemental analysis calcd (%) for $C_{56}H_{44}O_{16}P_4$ (1096.8): C 61.32, H 4.04; found C 61.06, H 4.37.

LSIMS: Experiments were performed with a Finnigan-MAT 95Q hybrid tandem mass spectrometer, with magnetic, electrostatic, and quadrupole analyzers mounted in series (BEQ geometry). An octapole collision cell was mounted between the electrostatic and the quadrupole analyzers and it was preceded by a series of focusing and deceleration lenses. Two detection systems, including a 30 keV conversion dynode and a multistage Philips electron-multiplier, were located after the electrostatic sector and after the quadrupole to perform MS and MS/MS experiments, respectively.

Each cavitand was dissolved in 3-NBA to give 2.8×10^{-3} M solutions. The five cavitands of series **5** and **6** were scarcely soluble in 3-NBA and were dissolved in glycerol at the same concentration. Solutions for all alkyl- and arylammonium ions were prepared from the corresponding chlorides, which were dissolved in 3-NBA at a concentration of 0.56 M. The samples subjected to LSIMS analysis were 1:1 mixtures of a cavitand and an alkylammonium chloride solutions that were shaken and then allowed to equilibrate for 10 min. The final concentrations of cavitands and candidate guests were 1.4×10^{-3} M and 0.28 M, respectively, except for the experiments in which the guest concentration was progressively varied to reach the final stoichiometric concentration. A droplet from these mixtures of cavitand and candidate guest was loaded onto the LSIMS probe tip, which was inserted into the ionization chamber and subjected to bombardment with Cs^+ ions.

The Cs^+-ion gun was operated at 30 keV collisional energy and 5 μA current. Sputtered ions were extracted from the ionization chamber and mass-analyzed by the magnetic sector under scanning. The scanned mass range started at least 200 Da below the mass of the protonated cavitand and ended 200 Da above the mass of the host–guest adduct. Ten mass spectra were averaged to produce the final data.

MS/MS: Proton affinities were determined by the "kinetic method". The ion corresponding to the proton-bound dimer was mass-selected by the magnet and subsequently decelerated to 70 eV. At this laboratory energy, the selected ions experienced multiple collisions with argon inside the octapole collision cell, which was maintained at a pressure of 0.15 Pa (1.5×10^{-3} mbar). The collision-induced decomposition products were determined by scanning the quadrupole mass analyzer over both large and narrow mass ranges. All the voltages of the lenses used in the MS/MS section of the instrument were optimized and scanned over the mass range under analysis. Lens adjustment at both low and high masses was executed just before the experiments in order to avoid any mass discrimination effect in the experiments where the decomposition products to be compared had widely separated masses (i.e., m/z 1153 for the protonated cavitand and m/z 74 for the diethylammonium ion).

Proton-bound dimers were produced both by LSIMS, by means of identical procedures to those cited above, or by chemical ionization. In the latter experiments, the alkylammonium ions were generated from the corresponding amines, whose vapors were transported in a small percentage from a vial by a flow of isobutane, used as the chemical ionization reagent gas. The pressure of the latter inside the ion source was 50 Pa (0.5 mbar). Triphenylphosphate was desorbed from an heated probe; cavitand **2b** was vaporized by a desorption chemical-ionization probe, by means of a fast heating ramp and cold ion-source to avoid thermal decomposition. Identical results were generated in the preparation of the proton-bound dimers by the two different methods.

Acknowledgements

E.D. acknowledges the Centro Interfacoltà di Misure "G. Casnati" of the University of Parma for instrumental facilities. Financial support from MURST (Rome) is gratefully acknowledged.

[1] a) *Host–Guest Complex Chemistry: Macrocycles* (Eds.: F. Vögtle, E. Weber), Springer, New York, **1988**; b) *Inclusion Phenomena and Molecular Recognition* (Ed.: J. L. Atwood), Plenum, New York, **1988**; c) D. J. Cram, J. M. Cram in *Container Molecules and Their Guests* (Ed.: J. F. Stoddard), Royal Society of Chemistry, London, **1994**; d) *Comprehensive Supramolecular Chemistry*, *Vols. 1 and 2* (Eds.: J.-M. Lehn, J. L. Atwood, J. E. D. Davies, D. D. MacNicol, G. W. Gokel, F. Vögtle), Pergamon, Oxford, **1996**.

[2] M. Vincenti, A. Irico, E. Dalcanale in *Advances in Mass Spectrometry*, *Vol. 14* (Eds.: E. J. Karijalainen, A. E. Hesso, J. E. Jalanen, U. P. Karijalainen), Elsevier Science, Amsterdam, **1998**, pp. 129–150.

[3] a) M. Vincenti, *J. Mass Spectrom.* **1995**, *30*, 925–939; b) J. S. Brodbelt, D. V. Dearden, in *Mass Spectrometry*, *Comprehensive Supramolecular Chemistry*, *Vol. 8* (Eds.: J. E. D. Davies, J. A. Ripmeester), Pergamon, Oxford, **1996**; c) K. Wang, G. W. Gokel, *Pure Appl. Chem.* **1996**, *68*, 1267–1272; d) C. A. Schalley, *Int. J. Mass Spectrom.* **2000**, *194*, 11–39.

[4] a) T. Lippmann, H. Wilde, M. Pinke, A. Schäfer, M. Hesse, G. Mann, *Angew. Chem.* **1993**, *105*, 1258–1260; *Angew. Chem. Int. Ed. Engl.* **1993**, *32*, 1195–1197; b) N. J. Haskins, M. R. Saunders, P. Camilleri, *Rapid Commun. Mass Spectrom.* **1994**, *8*, 423–426; c) R. Colton, S. Mitchell, J. C. Traeger, *Inorg. Chim. Acta* **1995**, *231*, 87–93; d) K. Wang, G. W. Gokel, *J. Org. Chem.* **1996**, *61*, 4693–4697; e) D.-S. Young, H.-Y Hung, L. L. Kao, *Rapid Commun. Mass Spectrom.* **1997**, *11*, 769–773; f) R. Bakhtiar, A. E. Kaifer, *Rapid Commun. Mass Spectrom.* **1998**, *12*, 111–114; g) C. A. Shalley, R. K. Castellano, M. S. Brody, D. M. Rudkevich, G. Siuzdak, J. Rebek, Jr., *J. Am. Chem. Soc.* **1999**, *121*, 4568–4579.

[5] a) L. M. Nuwaysir, J. A. Castoro, C. L.-C. Yang, C. L. Wilkins, *J. Am. Chem. Soc.* **1992**, *114*, 5748–5751; b) B. J. Goolsby, J. S. Brodbelt, E. Adou, M. Blanda, *Int. J. Mass Spectrom.* **1999**, *193*, 197–204.

[6] a) K. Laali, R. P. Lattimer, *J. Org. Chem.* **1989**, *54*, 496–498; b) S. Kurono, T. Hirano, K. Tsu-Jimoto, M. Ohashi, M. Yoneda, Y. Ohkawa, *Org. Mass Spectrom.* **1992**, *27*, 1157–1160; c) M. Sawada, M. Shizuma, Y, Takai, H. Yamada, T. Kaneda, T. Hanafusa, *J. Am. Chem. Soc.* **1992**, *114*, 4405–4406; d) G. J. Langley, J. D. Kilburn, S. S. Flack, *Org. Mass Spectrom.* **1993**, *28*, 478–480; e) S. Maleknia, J. S. Brodbelt, *J. Am. Chem. Soc.* **1993**, *115*, 2837–2843; f) M. Sawada, Y. Okumura, M. Shizuma, Y, Takai, Y. Hidaka, H. Yamada, T. Tanaka, T. Kaneda, K.Hirose, S. Misumi, S. Takahashi, *J. Am. Chem. Soc.* **1993**, *115*, 7381–7388; g) A. Mele, W. Panzeri, A. Selva, *Eur. Mass Spectrom.* **1997**, *3*, 347–354; h) K. B. Reiche, I. Starke, E. Kleinpeter, H.-J. Holdt, *Rapid Commun. Mass Spectrom.* **1998**, *12*, 1021–1027; i) M. Sawada, H. Yamaoka, Y. Takai, Y. Kawai, H. Yamada, T. Azuma, T. Fujioka, T. Tanaka, *Int. J. Mass Spectrom.* **1999**, *193*, 123–130.

[7] a) M. Meot-Ner, *J. Am. Chem. Soc.* **1983**, *105*, 4906–4911; b) A. K. Bose, O. Prakash, G. Y. Hu, J. Edasery, *J. Org. Chem.* **1983**, *48*, 1782–1784; c) R. B. Sharma, A. T. Blades, P. Kebarle, *J. Am. Chem. Soc.* **1984**, *106*, 510–516; d) C.-C. Liou, J. S. Brodbelt, *J. Am. Chem. Soc.* **1992**, *114*, 6761–6764; e) H. -F. Wu, J. S. Brodbelt, *J. Am. Soc. Mass Spectrom.* **1993**, *4*, 718–722.

[8] a) H. -F. Wu, J. S. Brodbelt, *J. Am. Chem. Soc.* **1994**, *116*, 6418–6426; b) E. J. Alvarez, V. H. Vartanian, J. S. Brodbelt, *J. Am. Soc. Mass Spectrom.* **1997**, *8*, 620–629; c) S. M. Blair, E. C. Kempen, J. S. Brodbelt, *J. Am. Soc. Mass Spectrom.* **1998**, *9*, 1049–1059; d) S. M. Blair, J. S. Brodbelt, G. M. Reddy, A. P. Marchand, *J. Mass Spectrom.* **1998**, *33*, 721–728;

[9] a) H. Zhang, I.-H. Chu, S. Leming, D. V. Dearden, *J. Am. Chem. Soc.* **1991**, *113*, 7415–7417; b) I.-H. Chu, H. Zhang, D. V. Dearden, *J. Am. Chem. Soc.* **1993**, *115*, 5736–5744; c) I.-H. Chu, D. V. Dearden, *J. Am. Chem. Soc.* **1995**, *117*, 8197–8203; d) Q. Chen, K. Cannell, J. Niccoll, D. V. Dearden, *J. Am. Chem. Soc.* **1996**, *118*, 6335–6341; e) P. S. H. Wong, H.-J. Yu, D. V. Dearden, *Inorg. Chim. Acta* **1996**, *246*, 259–265; f) D. V. Dearden, C. Dejsupa, Y. Liang, J. S. Bradshow, R. M. Izatt, *J. Am. Chem. Soc.* **1997**, *119*, 353–359; g) K. A. Kellersberg, C. Dejsupa, Y.-Y. Liang, R. M. Pope, D. V. Dearden, *Int. J. Mass Spectrom.* **1999**, *193*, 181–195.

[10] a) M. Vincenti, E. Dalcanale, P. Soncini, G. Guglielmetti, *J. Am. Chem. Soc.* **1990**, *112*, 445–447; b) M. Vincenti, E. Pelizzetti, E. Dalcanale, P. Soncini, *Pure Appl. Chem.* **1993**, *65*, 1507–1512; c) M. Vincenti, E. Pelizzetti, E. Dalcanale, P. Soncini, *Pure Appl. Chem.* **1995**, *67*, 1075–1084; d) A. Arduini, M. Cantoni, E. Graviani, A. Pochini, A. Secchi, A. R. Sicuri, R. Ungaro, M. Vincenti, *Tetrahedron* **1995**, *51*, 599–606; e) M. Vincenti, E. Dalcanale, *J. Chem. Soc. Perkin Trans. 2* **1995**, 1969–1976.

[11] a) T. Lippman, H. Wilde, E. Dalcanale, L. Mavilla, G. Mann, U. Heier, S. Spera, *J. Org. Chem.* **1995**, *60*, 235–242; b) P. Delangle, J.-P. Dutasta, *Tetrahedron Lett.* **1995**, *36*, 9325–9328.

[12] For a review on in–out isomerism see: R. W. Alder, S. P. East, *Chem. Rev.* **1996**, *96*, 2097–2111.

[13] J. M. J. Nuutinen, A. Irico, M. Vincenti, E. Dalcanale, J. M. H. Pakarinen, P. Vainiotalo, *J. Am. Chem. Soc.* **2000**, *122*, 10090–10100.

[14] T. Lippmann, E. Dalcanale, G. Mann, *Tetrahedron Lett.* **1994**, *35*, 1685–1688.

[15] a) J. Pierce, K. L. Busch, R. A. Walton, R. G. Cooks, *J. Am. Chem. Soc.* **1981**, *103*, 2583–2588; b) K. L. Busch, S. E. Unger, A. Vincze, R. G. Cooks, T. Keough, *J. Am. Chem. Soc.* **1982**, *104*, 1507–1511; c) R. A. W. Johnstone, I. A. S. Lewis, M. E. Rose, *Tetrahedron* **1983**, *39*, 1587–1603; d) G. Bonas, C. Sosso, M. R. Vignon, *J. Inclus. Phenom. Mol. Recog. Chem.* **1989**, *7*, 637–647; e) J. M. Miller, K. Balasanmugam, A. Fulcher, *Org. Mass Spectrom.* **1989**, *24*, 497–503; f) T. Takahashi, A. Uchiyama, K. Yamada, B. C. Lynn, G. W. Gokel, *Tetrahedron Lett.* **1992**, *33*, 3825–3828; g) J. B. Cunniff, P. Vouros, D. L. Kaplan, S. A. Fossey, *J. Am. Soc. Mass Spectrom.* **1994**, *5*, 638–648.

[16] a) F. Inouchi, K. Araki, S. Shinkai, *Chem. Lett.* **1994**, 1383–1386; b) F. Inouchi, Y. Mihara, T. Inazu, S. Shinkai, *Angew. Chem.* **1995**, *107*, 1459–1462; *Angew. Chem. Int. Ed. Engl.* **1995**, *34*, 1364–1366.

[17] E. Dalcanale, P. Jacopozzi, F. Ugozzoli, G. Mann, *Supramol. Chem.* **1998**, *9*, 305–316.

[18] *Handbook of Chemistry and Physics*, 73rd ed. (Ed. D. L. Lide), CRC, Boca Raton, **1992**, Chapter 9, p. 53.

[19] K. D. Cook, P. J. Todd, D. H. Friar, *Biomed. Environ. Mass Spectrom.* **1989**, *18*, 492–497.

[20] a) R. G. Cooks, T. L. Kruger, *J. Am. Chem. Soc.* **1977**, *99*, 1279–1281; b) S. A. McLuckey, D. Cameron, R. G. Cooks, *J. Am. Chem. Soc.* **1981**, *103*, 1313–1317.

[21] E. P. Hunter, S. G. Lias, *J. Phys. Chem. Ref. Data* **1998**, *27*, 413.

[22] a) E. Dalcanale, J. Hartmann, *Sens. Actuators B* **1995**, 24–25; b) E. Dalcanale, J. Hartmann, *Sens. Actuators B* **1995**, 39–42.

[23] R. Pinalli, F. F. Nachtigall, F. Ugozzoli, E. Dalcanale, *Angew. Chem.* **1999**, *111*, 2530–2533; *Angew. Chem. Int. Ed.* **1999**, 38, 2377–2380.

Received: October 12, 2000 [F2794]

  0947-6539/01/0709-2042 $ 17.50+.50/0